The Charge Density in Dichlorotetrakis(thiourea)nickel(II), $[Ni\{SC(NH_2)_2\}_4Cl_2]$: a Contrast between Spectroscopy and Diffraction†

Brian N. Figgis* and Philip A. Reynolds
School of Chemistry, University of Western Australia, Nedlands, Australia 6009

The charge density observed by *X*-ray diffraction at 140 K in $[Ni(tu)_4Cl_2]$ (tu = thiourea) is reported. The values for the chloride, thiourea, and Ni^{II} fragments closely resemble those of the free ion or molecule, except (*a*) each chloride σ-donates 0.16(14) e and π-donates 0.35(15) e; (*b*) each thiourea σ-donates 0.17(20) e to the nickel; (*c*) Ni^{II}, in its $^3B_1$ ground state, has a 3*d* configuration $d_{xy}^{1.91(14)}$, $d_{xz,yz}^{3.08(18)}$, $d_{x^2-y^2}^{1.12(14)}$, $d_{z^2}^{1.39(14)}$ with a substantial [1.6(7) e] 4*p* population. These figures are consistent with a conventional bonding model, in which $3d_\sigma$ orbitals on Ni^{II} σ-bond almost equally to chlorine and thiourea, and in which $3d_\pi$ *and* $4p_\pi$ orbitals π-bond only to chlorine. The residual density maps suggest a differential nephelauxetic effect is occuring, with metal-centred π orbitals larger than σ. A polarisation of the entire $NiCl_2$ fragment is also observed, perhaps caused by intermolecular effects. Previous results show that thiourea has a much larger effect on the spectra and magnetism than the chloride. This contrast with the charge-density results is explained by the greater dominance of overlap in spectroscopy, and of ligand energy levels (or crudely, ionisation potentials) in charge densities. This illustrates experimentally the theoretical observation that covalence (*i.e.* molecular orbital) parameters are best 'directly' observed by diffraction, since spectroscopy is often dominated in more ionic complexes by the less interesting terms due to orthogonalisation of metal and ligand orbitals.

Our previous spin and charge density studies on $[Ni(NH_3)_4(NO_2)_2]$ have shown that while simple ligand-field theory is a reasonable qualitative description of the bonding, some of the observed features are puzzling and the theory is quantitatively inadequate.[1,2] A second experiment on a tetragonal Ni^{II} complex seems called for to try to distinguish between the inadequacy, if any, of simple theories of bonding in the isolated complex molecule and complicating effects such as intermolecular forces and experimental artefacts.

Dichlorotetrakis(thiourea)nickel(II), $[Ni(tu)_4Cl_2]$, has a very simple crystal structure (11 independent atoms)[3,4] involving two independent *trans*-Ni–Cl bonds and four equivalent Ni–tu equatorial bonds. Spectroscopic[5,6] and magnetic[5,7] properties are known for the compound and have been interpreted by Gerloch *et al.*[5] in terms of a crystal-field model. Such an ionic model does not necessarily imply ionic bonding; it tells us about the *covalent* bonding, and it can indeed be recast in terms of the *explicitly* covalent angular-overlap model for example.[8] It is interesting to compare and contrast the information on covalence obtained by spectroscopy with that from diffraction. Comparison of the charge density of bonded thiourea with that obtained in crystalline thiourea itself[9,10] is also of some interest.

The two Ni–Cl bonds are of markedly different length (240 and 252 pm). The idea of independent, transferrable bond properties is an old, and successful, idea of structural chemists; any differences here may illuminate the inherent limitations of this idea.

While these stable, easily grown, simple crystals of $[Ni(tu)_4Cl_2]$ give the excellent quality diffraction data necessary for charge-density studies, the crystal space group is non-centrosymmetric and this may limit interpretation. Construction of model-independent electron-density difference maps is impossible, necessitating detailed modelling. In addition, the errors in derived parameters are double those in the centrosymmetric case.[11]

In this paper we initially present the experimental details and derive structural and thermal parameters for the molecule. Using these we then model the charge density with spherical and aspherical valence and then multipole models, discussing the fit and the remaining residual charge density.

Experimental

Crystals of $[Ni(tu)_4Cl_2]$ were prepared by slow evaporation of an aqueous solution of thiourea containing a substantial excess of nickel(II) chloride.[5] Crystals grew as tetragonal prisms along [001]. Relatively isotropic crystals with habit {110} and {001} were selected for the *X*-ray diffraction experiments. After initial *X*-ray photography in a Weissenberg camera they were mounted on a Syntex $P2_1$ four-circle diffractometer and two data sets were collected at 140(5) and 295(1) K. The estimated standard deviation (e.s.d.) of 5 K for the former reflects not the stability of the temperature, which was better than 2 K, but the absolute value. The tetragonal cell constants were determined by a least-squares fitting of the setting angles of six reflections in each case. At 140(5) K a complete sphere of data, using Mo-K_α radiation, was collected to a 2θ of 30° and two octants, *hkl* and $\bar{h}k\bar{l}$, to a 2θ maximum of 85°. The experimental conditions (scan widths, *etc.*) have been described previously.[1] Standard intensities fell by *ca.* 2% at 140 K and by *ca.* 6% at 295 K over the data collection period. At 140 K the two octants were taken consecutively, and at 295 K the data were collected in *h* layers. In this latter case the tetragonal equivalents were spread through the data collection. Crystal and experimental data are given in Table 1. After correction for standards the data at 140 K were corrected for absorption with the program ABSCOR of the X-RAY 76 system.[12] At 140 K for $2\theta < 30°$ the agreement factor between the four, non-centrosymmetric tetragonal, equivalents was $R = \Sigma Av(|I - Av(I)|)\Sigma Av(I) = 0.014$ (Av = arithmetic average). This excellent agreement supported

† *Supplementary data available* (No. SUP 56292, 5 pp.): thermal parameters. See Instructions for Authors, *J. Chem. Soc., Dalton Trans.*, 1986, Issue 1, xvii—xx. Structure factors are available from the editorial office.

Non-S.I. unit employed: eV ≈ 1.60 × 10^{-19} J.

Table 1. Crystal data and experimental conditions*

Temperature (K)	140(5)		295(1)
Crystal dimenstions (mm)	0.28	(110) to ($\bar{1}\bar{1}$0)	0.40
	0.28	(1$\bar{1}$0) to ($\bar{1}$10)	0.40
	0.30	(001) to (00$\bar{1}$)	0.40
Space group		*I*4	
Unit cell: *a*/Å	9.559(5)		9.606(2)
c/Å	8.974(5)		9.083(2)
U/Å^3	820(1)		838.1(6)
No. of reflections measured	1 991		11 040
No. of unique reflections	1 598		3 043
$(\sin\theta/\lambda)_{max.}$/nm^{-1}	9.07		1.53
μ(Mo-K_α)/mm^{-1}	1.98		9.94
Transmission factor	0.593—0.633		—

* Mo-K_α radiation (λ = 0.710 69 Å).

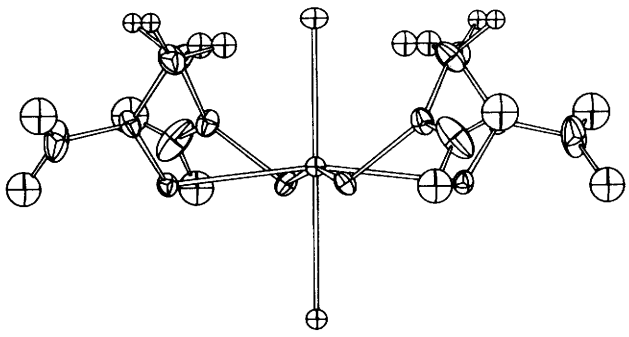

Figure 1. An ORTEP drawing of [Ni(tu)$_4$Cl$_2$] (140 K parameters). The Cl(1)–Ni–Cl(2) four-fold axis is vertical; thermal ellipsoids are drawn at the 50% probability level

Table 2. Relative atomic co-ordinates ($\times 10^4$) with e.s.d.s in parentheses*

Atom	*x*	*y*	*z*	Atom	*x*	*y*	*z*
Ni(1)	0	0	0	N(2)	2 071(2)	2 614(2)	−1 934(2)
	0	0	0		2 080(2)	2 604(2)	−1 957(2)
	0	0	0		2 082(2)	2 603(2)	−1 958(2)
Cl(1)	0	0	−2 646(1)	H(1)	1 620(26)	4 932(25)	0 258(26)
	0	0	−2 677(1)		1 645(29)	5 031(29)	0 284(42)
	0	0	−2 678(1)		1 732(—)	5 012(—)	0 299(—)
Cl(2)	0	0	2 771(1)	H(2)	2 644(35)	4 712(38)	−0 777(37)
	0	0	2 785(1)		2 575(43)	4 875(46)	−0 847(42)
	0	0	2 785(1)		2 629(—)	4 816(—)	−0 884(—)
S(1)	0 303(1)	2 535(1)	0 318(1)	H(3)	2 684(31)	2 963(27)	−2 512(29)
	0 281(1)	2 541(1)	0 313(1)		2 692(38)	2 872(31)	−2 583(37)
	0 281(1)	2 541(1)	0 311(1)		2 700(—)	2 811(—)	−2 424(—)
C(1)	1 541(1)	3 271(1)	−0 794(2)	H(4)	1 786(35)	1 774(36)	−2 250(37)
	1 536(2)	3 283(2)	−0 809(2)		1 791(32)	1 785(31)	−2 187(33)
	1 538(2)	3 281(2)	−0 808(2)		1 776(—)	1 704(—)	−2 147(—)
N(1)	1 983(2)	4 543(2)	−0 492(3)				
	1 977(2)	4 565(2)	−0 507(3)				
	1 980(3)	4 571(2)	−0 505(4)				

* The first row are the data at 295 K, the second the X-RAY 76 results (140 K), and the third the high-angle ASRED refinement results.

assignment of a tetragonal space group. The Friedel pair agreement was about 0.035 showing obvious effects of dispersion in a non-centrosymmetric space group. Absences $h + k + l$ odd were checked and were not significant, indicating an *I*-centred cell, and a space group of *I*4, $I\bar{4}$, or *I*4/*m*. For the complete set of reflections at 140 K, $\Sigma\sigma(I)/I$ was 0.014. These two measures of data quality are rather better than our normal values of *ca.* 0.020 in simple metal complexes which give good charge densities, and lead us to be confident of our accuracy here. The data at 295 K were not analysed in such detail, since only approximate parameters are required, but an inspection shows the data are also of better quality than usual. The absorption ($\mu r \sim 0.8$) was small, and since the crystal was mounted in a general orientation, the good agreement of equivalents indicated that an absorption correction was not warranted at 295 K, where charge densities were not to be analysed.

Least-squares Refinement.—Three different types of refinement have been performed. Initially, traditional, spherical neutral-atom refinements were used to investigate structure and thermal motion; then 'valence' refinements to investigate the bonding effects on the charge density; finally a multipole refinement of the data was performed.

Structure and thermal motion refinements. Least-squares refinement of atomic co-ordinates and anisotropic thermal parameters (for atoms other than H) and an isotropic extinction parameter were performed on both data sets by use of program CRYLSQ in the full-matrix mode from the X-RAY 76 program system.[12] Neutral-atom scattering factors were used[13,14] and were modified, except for H, for anomalous dispersion.[15] The function $\Sigma[\sigma^2(F_o)]^{-1}(|F_o| - |F_c|)^2$ was minimised for those reflections with $I > 3\sigma(I)$. Starting parameters were taken from Lopez-Castro and Truter.[3] The correct enantiomorph gave $R(F) = \Sigma||F_o| - |F_c||/\Sigma|F_o| = 0.021$ and $R'(F) = \Sigma[\sigma(F_o)]^{-1}||F_o| - |F_c||/\Sigma[\sigma(F_o)]^{-1}|F_o| = 0.029$ for the 1 512 'observed' data (140 K) with the 62 variables. The opposite enantiomorph gave *R* factors higher by 0.02. At 295 K the 2 492 'observed' data gave $R(F) = 0.022$ and $R'(F) = 0.029$. The derived positional parameters are listed in Table 2. The extinction in the data at 140 K was significant although small: a maximum reduction of 4% in intensity. At 295 K the extinction was substantially larger: up to a 14% intensity reduction. The positional parameters are in good agreement with those of Lopez-Castro and Truter.[3] Their precision is 5—10 times less than ours, not unexpected given their use of photographic data and the large absorption correction necessary when using Cu-K_α radiation (final *R* factor of 0.07). Their thermal parameters, if multiplied by (140/110) to take account of the temperature difference, are also in good agreement with ours.

Selected intramolecular distances and angles, both at 140 and 295 K, are given in Table 3. Intermolecular geometry is summarised by Table 4. The molecular geometry at 140 K is illustrated by the ORTEP diagram of Figure 1.

Valence orbital refinement. Since bonding undoubtedly modifies the form-factors of the valence electrons, we have performed a refinement of high-angle data only ($\sin\theta/\lambda > 5.0$ nm^{-1}), using all data at 140 K and minimising $\Sigma[\sigma^2(I_o)]^{-1}(I_o - I_c)^2$ using the local program ASRED.[1] This procedure, being less sensitive to valence electrons, allows a more reliable estimate of the core-electron thermal motion if not affected by anharmonicity. Hydrogen-atom thermal and positional parameters were kept fixed at values previously determined by refinement of all the data by ASRED, since these are ill determined by high-angle data alone. The parameter values are also listed in Table 2. The 1 166 data (n.o.) gave $R(I) = 0.036$, $R'(I) = 0.058$, and $\chi = \{\Sigma[\sigma^2(I_o)]^{-1}(I_o - I_c)^2/(\text{n.o.} - \text{n.v.})\}^{\frac{1}{2}} = 1.53$ for the 45 variables (n.v.). With a $3\sigma(I)$ data cut-off imposed this would correspond to $R(F) = 0.025$ for 1 112 reflections.

The derived thermal and positional parameters do not differ significantly from the values obtained in the standard structural refinement. In this case, somewhat unusually, it appears that the biasing effects of data exclusion, refinement on F and valence effects are negligible. It does however give us confidence in the thermal parameters.

We have used these thermal and positional parameters in an initial estimate of the valence effects by use of Fourier maps. Three deformation density maps are presented in Figure 2(*a*)—(*c*). Figure 2(*a*) shows the Ni(1)Cl(1)Cl(2)S(1) plane, (*b*) the Ni(1)S(1)S(2) plane, and (*c*) the S(1)C(1)N(1)N(2) least-squares plane. S(2) is the sulphur atom related to S(1) by a 90° rotation about *c*. In Figure 2(*a*) the atoms are, by symmetry, exactly coplanar; while in Figure 2(*c*) the atoms of the thiourea molecule are almost coplanar (maximum deviation 0.4 pm). In order to construct these maps we have used $|F_o|$, $|F_c|$ and the theoretical phases. The theoretical values were calculated by use of the high-angle parameters. Use of theoretical phases for a non-centrosymmetric crystal means, of course, that our deformation density is model dependent.

Improvement of the model to minimise this model-dependent error must start with an improved description of the valence-electron form factors. We shall model the valence electrons as hybridised atomic orbitals each with a refinable electron occupation number. This anisotropic valence model has been

Table 3. Selected intramolecular interatomic distances (Å) and bond angles (°) with e.s.d.s in parentheses

	295 K	140 K
Bond lengths		
Ni(1)–Cl(1)	2.403(1)	2.402(2)
Ni(1)–Cl(2)	2.517(1)	2.500(2)
Ni(1)–S(1)	2.469(1)	2.460(1)
C(1)–S(1)	1.713(2)	1.719(2)
N(1)–C(1)	1.322(2)	1.324(3)
N(2)–C(1)	1.316(2)	1.324(3)
N(1)–H(1)	0.85(3)	0.90(3)
N(1)–H(2)	0.70(3)	0.71(4)
N(2)–H(3)	0.86(3)	0.85(3)
N(2)–H(4)	0.90(3)	0.96(3)
Bond angles		
Cl(1)–Ni(1)–S(1)	96.72(1)	96.55(1)
S(1)–Ni(1)–S(1^{I})	166.57(4)	166.91(5)
S(1)–Ni(1)–S(1^{II})	89.22(2)	89.26(2)
Ni(1)–S(1)–C(1)	114.84(5)	114.63(6)
S(1)–C(1)–N(1)	118.8(2)	119.0(2)
S(1)–C(1)–N(2)	122.3(1)	121.8(1)
N(1)–C(1)–N(2)	118.8(2)	119.2(2)
H(1)–N(1)–C(1)	116(2)	121(2)
H(2)–N(1)–C(1)	115(3)	124(3)
H(1)–N(1)–H(2)	124(3)	115(4)
H(3)–N(2)–C(1)	124(2)	129(2)
H(4)–N(2)–C(1)	124(2)	121(2)
H(3)–N(2)–H(4)	111(3)	110(3)

Symmetry codes: I $-x, -y, z$; II $-y, x, z$.

Table 4. Selected non-bonded lengths (Å) and angles (°) with e.s.d.s in parentheses

	295 K	140 K
Lengths		
Cl(1) · · · N(2)	3.268(2)	3.250(2)
Cl(1) · · · H(4)	2.44(4)	2.46(3)
Cl(2) · · · N(1)	3.329(3)	3.297(3)
Cl(2) · · · H(2^{I})	2.63(3)	2.63(4)
S(1) · · · N(2^{I})	3.551(2)	3.520(2)
S(1) · · · H(3^{I})	2.80(3)	2.73(4)
Angles		
Cl(1) · · · H(4^{I})–N(2^{I})	153(8)	153(10)
Cl(2) · · · H(2^{I})–N(1^{I})	177(24)	157(14)
S(1) · · · H(3^{I})–N(2^{I})	147(8)	155(11)

Symmetry code: I $\frac{1}{2} + x, \frac{1}{2} + y, \frac{1}{2} + z$.

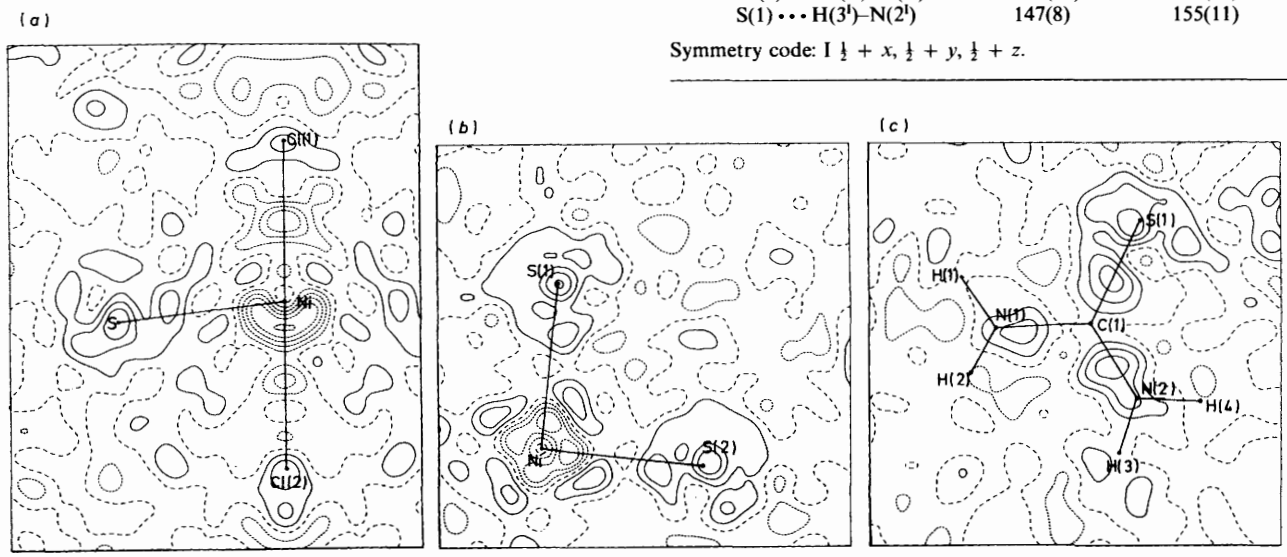

Figure 2. Residual electron density obtained by use of spherical 'free' atom model. Contour interval 100 e nm^{-3}; (——) positive, (· · · ·) negative, (— — —) zero. (*a*) $NiCl_2S$ plane; (*b*) NiS_2 plane; (*c*) thiourea plane

Table 5. Valence hybrid-orbital model derived population and radial parameters with e.s.d.s in parentheses

(*a*) Population parameters

Ni(1)	$3d_{xy}$	1.91(14)	S(1)	$(sp^3)_1$	1.41(4)
	$3d_{xz,yz}$	3.08(18)		$(sp^3)_2$	1.45(5)
	$3d_{x^2-y^2}$	1.12(14)		$(sp^3)_3$	1.57(5)
	$3d_{z^2}$	1.39(14)		$(sp^3)_4$	1.74(5)
	$4(sp)_1$	0.8(5)	C(1)	$(sp^2)_1$	1.05(7)
	$4(sp)_2$	−0.2(5)		$(sp^2)_2$	0.78(9)
	$4p_{x,y}$	1.6(7)		$(sp^2)_3$	0.98(10)
Cl(1)	$(sp)_1$	2.21(12)		p_π	0.59(7)
	$(sp)_2$	1.55(11)	N(1)	$(sp^2)_1$	1.69(8)
	$p_{x,y}$	3.46(15)		$(sp^2)_2$	1.32(8)
Cl(2)	$(sp)_1$	1.70(12)		$(sp^2)_3$	1.37(8)
	$(sp)_2$	2.21(11)		p_π	1.35(8)
	p_{xy}	3.84(15)	N(2)	$(sp^2)_1$	1.48(8)
				$(sp^2)_2$	1.42(8)
				$(sp^2)_3$	1.53(6)
				p_π	1.43(7)
			H(1)	1*s*	0.75(6)
			H(2)	1*s*	0.62(10)
			H(3)	1*s*	0.59(5)
			H(4)	1*s*	0.71(9)

(*b*) Radial and other parameters

Ni(1)	θ_D(°)	6(6)	S(1)		
	radius 3*d* 1.01(1)			radius 3*sp* 0.938(6)	
Cl(1)			C(1)		
	radius 3*sp* 0.94(1)			radius 2*sp* 0.91(3)	
Cl(2)			N(1)		
	radius 3*sp* 0.99(1)			radius 2*sp* 1.01(1)	
			N(2)		
				radius 2*sp* 1.02(1)	
H(1)	*U*	0.038(12)	H(3)	*U*	0.021(12)
H(2)	*U*	0.012(27)	H(4)	*U*	0.010(13)

set out in detail elsewhere.[1] Here we will only note the conditions peculiar to this crystal.

The thiourea molecule valence density has been represented as *s*–*p* hybrids. We have put on each H a 1*s* orbital; on each of the three N $2s2p^2$ hybrids and a $2p_\pi$ orbital with $(sp^2)_1$ directed at C(1) and $(sp^2)_{2,3}$ approximately directed at H(1) and H(3) for N(1) and N(2) respectively. On C(1) we place three $2s2p^2$ hybrids and a $2p_\pi$ orbital with $(sp^2)_1$ directed at S(1) and $(sp^2)_2$ and $(sp^2)_3$ approximately directed at N(1) and N(2); on S(1) four $3s3p^3$ hybrids with $(sp^3)_1$ directed at Ni(1) with $(sp^3)_2$ approximately directed at C(1).

The $NiCl_2$ linear fragment lies on the crystal four-fold axis. The chlorines have been given two $3s3p$ hybrids and a degenerate $3p_\pi$ pair of orbitals, $(sp)_1$ being directed towards Ni(1) in each case. On the nickel we have placed the most general $3d$ combinations consistent with symmetry, together with two $4s4p$ and two $4p_\pi$ orbitals with $(sp)_1$ directed towards Cl(2). This most general $3d$ orbital combination requires five parameters. In the 4 site symmetry the centrosymmetric $3d$ orbitals give four sets of orbitals: $A(3d_{z^2}) + E(3d_{xz,yz}) + 2B(3d_{xy}$ and $3d_{x^2-y^2})$. For an arbitrary choice of x axis we thus have four $3d$ populations and a term $\langle 3d_{xy}|3d_{x^2-y^2}\rangle$ reflecting the mixing of these two orbitals in the arbitrary axis systems we have chosen. It is convenient, since it is homogeneous, to refine using these five population parameters. However, in presenting the results we have quoted four populations, and an angle θ_D; θ_D is the angle of rotation required from the direction defined by the ligating sulphur atoms to that where $3d_{xy}/3d_{x^2-y^2}$ mixing is zero, *i.e.* θ_D defines the natural axes of quantisation of the *d* orbitals on the nickel. There remain only four population parameters: $3d_{z^2}$, $3d_{xz,yz}$, $3d_{xy}$, and $3d_{x^2-y^2}$.

Table 6. Net charges obtained in the valence and multipole refinements with e.s.d.s in parentheses

Atom	Valence	Multipole
Ni(1)	+0.30(20)	−0.16(30)
[Cl(1) + Cl(2)]/2	−0.48(18)	−0.47(11)
S(1)	−0.17(10)	−0.06(12)
C(1)	+0.60(13)	+0.04(14)
N(1)	−0.73(12)	−0.60(14)
N(2)	−0.86(12)	−0.72(14)
H(1)	0.25(6)	+0.41(4)
H(2)	0.38(10)	+0.43(17)
H(3)	0.41(5)	+0.48(5)
H(4)	0.29(9)	+0.33(6)
thiourea	+0.17(20)	+0.28(20)

This set of hybrid orbitals and associated refinable population parameters is sufficient to describe a conventional ligand-field model of the electron density if we neglect overlap features. However, it is well known that crystal-field effects can cause radial expansion or contraction of the constituent atomic orbitals. To accommodate this we have included refinable parameters on each atom κ_{nl}. The form factor used for an *nl* hybrid is given by $f_{nl}(\kappa_{nl}S)$ where S is the wavevector and $f_{nl}(S)$ the theoretical form-factor at that wavevector.

Using ASRED, with fixed non-hydrogen atom positions and thermal parameters, the valence form factors were refined, using all data, minimising the function $\Sigma[\sigma^2(I_o)]^{-1}(I_o - I_c)^2$. For the hydrogen atoms, besides the 1*s* population, *x*, *y*, *z*, and *U* were also simultaneously refined. The valence-electron scattering curves used were those for Ni^{2+}, Cl^-, S, C, N, and H tabulated in 'International Tables'.[16] The 1 598 data gave $R(I) = 0.025$, $R'(I) = 0.048$, and $\chi = 1.78$ for the 58 variables. The starting spherical theoretical atom values were $R(I) = 0.037$, $R'(I) = 0.058$, and $\chi = 2.17$. Crystal electroneutrality was constrained during the refinement. In other cases[1,17] this constraint has caused severe bias in the derived parameters. In this case relaxation of electroneutrality gave $F(000)_{derived} = 0.980$ $F(000)_{theory}$, together with almost no change in the refinement, showing that in this case no appreciable bias is caused. Hydrogen radial parameters were fixed at 1.0 as these were found to be highly correlated with the thermal parameter. This implies that the $\bar{U}$ for hydrogen atoms is a measure of the *size* of the form factor as well as thermal motion.

The derived values of valence parameters are listed in Table 5. We have omitted the hydrogen positional parameters, which did not change by large amounts. Net charges are given in Table 6.

There were no highly correlated parameters except between the various multipole totals on Cl(1) and Cl(2) where coefficients are *ca.* −0.8. This correlation is maintained in all subsequent refinements. As a consequence while the mean Cl multipole populations *are* well defined, the individual populations are *not*. We may speculate that this is a consequence of non-centrosymmetry: Cl(1) and Cl(2) are almost exactly related by inversion through Ni (as no other atoms are). The difference between them is thus very sensitive to the imaginary part of the structure factor, which is independent of Ni *and* more model dependent than the real part. We must therefore conclude that any differences in Ni–Cl bond lengths are *not* significant in this experiment due to the large uncertainities in the relevant parameters.

Figure 3(*a*)—(*c*) shows the same sections of Fourier difference density as 2(*a*)—(*c*), but this time the residual densities remaining after subtraction of the 'observed' and calculated densities (using valence model phases for both) are calculated. In addition, a refinement was performed in which the individual

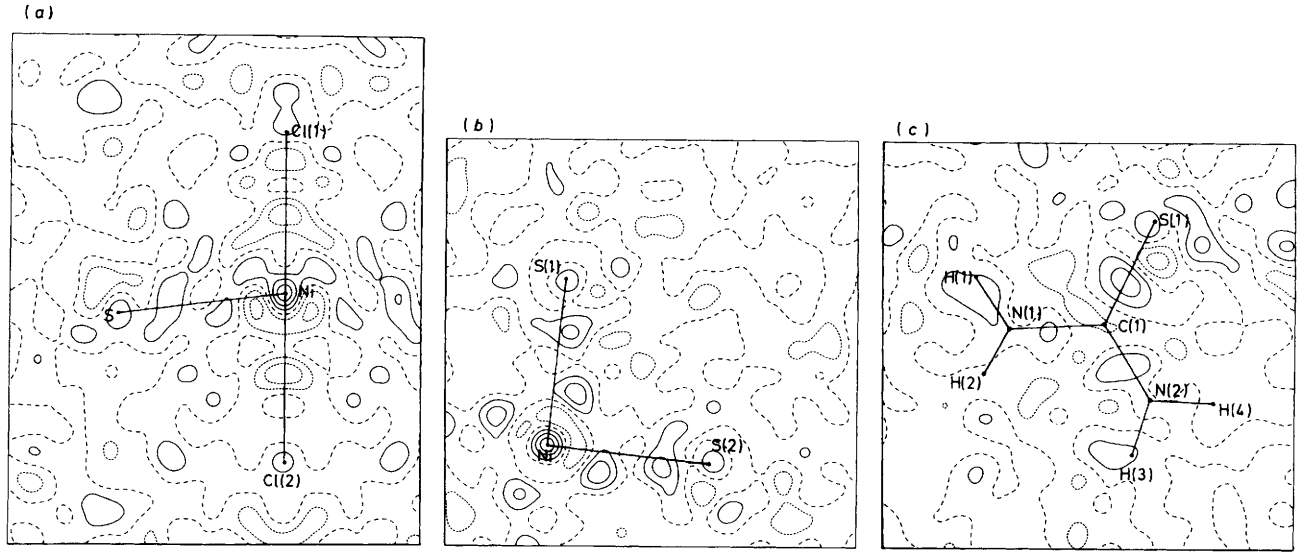

Figure 3. Residual electron density obtained by use of the valence-electron refinement; details are as in Figure 2

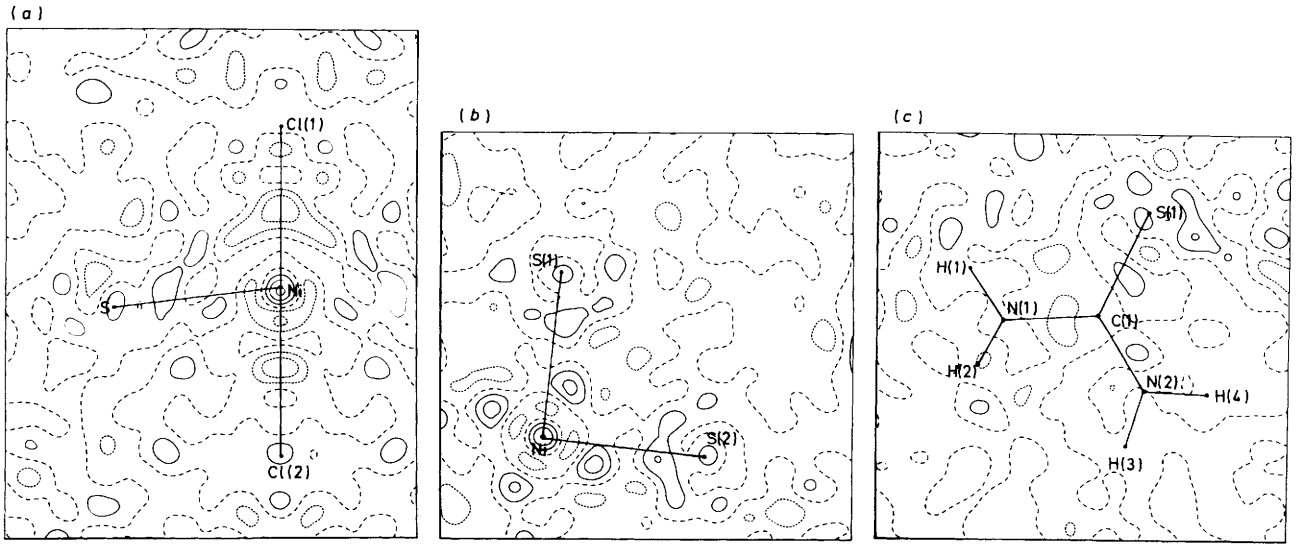

Figure 4. Residual electron density obtained by use of the multipole refinement; details are as in Figure 2

orbital population parameters were constrained so that each atom had a spherical electron density. The resulting net charges are also listed in Table 6.

Multipole refinement. As the Fourier maps show, the valence-orbital model is not a complete description of the observed structure factors. An improved model requires more terms. Although it is possible to add more valence terms, for example $3s$–$3p$–$3d$ hybrids on the sulphur atom, it is simpler to recast the model in multipole form and later discuss any orbital implications of the multipoles. As in all multipole models we must choose the angular flexibility (*i.e.* which multipoles), and also the radial flexibility. We chose multipoles consistent with both Mullen's thiourea refinement,[9] and our valence model: that is, up to order 4 on Ni, Cl, and S; order 3 on C and N; and order 2 on H. We use the natural definition of the spherical harmonics of Condon and Shortley[18] which differs from most others by a factor of $(-1)^m$ for Y_l^m with $m > 0$. Apart from the crystallographic four-fold axis through $NiCl_2$ we also impose non-crystallographic constraints on the thiourea molecule of a mirror plane in the thiourea plane, and of cylindrical symmetry about all C–H bonds. This reduces the number of independent multipoles from 130 to 78.

The radial terms in most multipole refinements are based on Hirshfeld's treatment[19] in which different orders of multipoles for a given atom can have *different* radial dependences which are related *via* a common 'atomic exponent'. Although this provides good fits for first row molecules, it is somewhat arbitrary.

To maintain contact with our valence model we will use the same radial dependence of electron density for all multipoles. This will give the higher multipoles more contracted distributions than the Hirshfeld choice. To increase radial flexibility we will retain κ_{nl} as refinable parameters. We will use radial dependences of $3d$, $3p$, $3p$, $2p$, $2p$, and $1s$ for Ni, Cl, S, C, N, and H respectively. The extra radial integrals required in the form factors were calculated from Clementi and Roetti[20] wave-

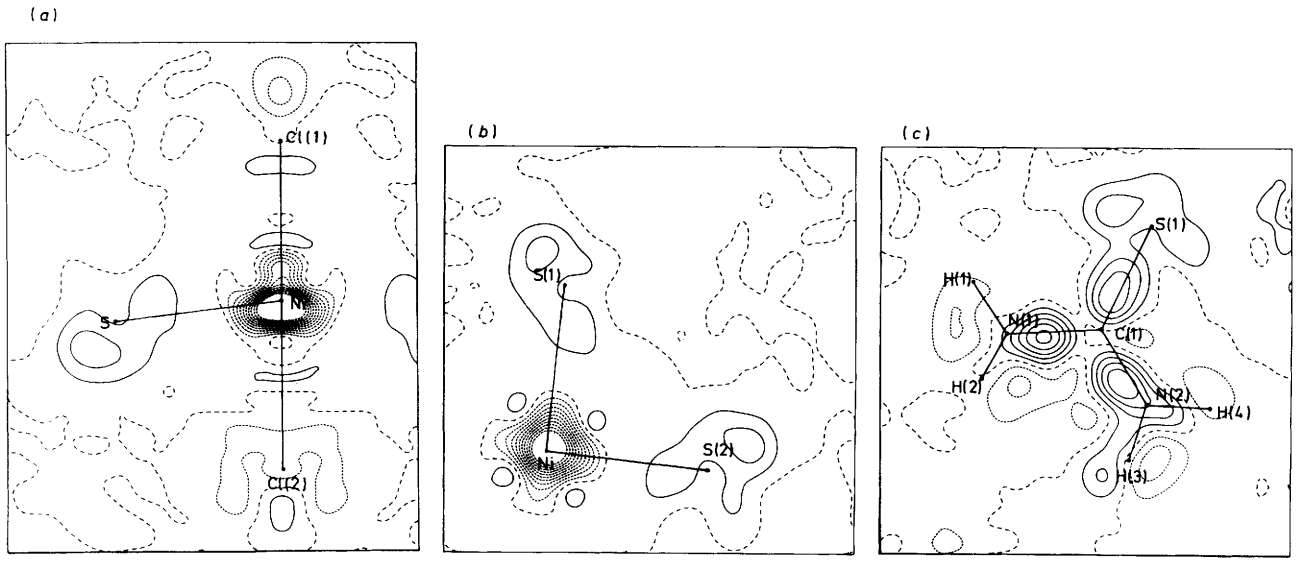

Figure 5. Deformation electron density estimated from multipole model; details are as in Figure 2

functions by the local program JCALC.[17] The integrals already in use from International Tables[16] were not changed, so as to provide maximum comparability between multipole and valence refinement. We note that the two sets of form factors differ insignificantly where both exist. In addition to these multipoles we have also put an electron density up to multipole order three on nickel with a 4*p* radial dependence, calculated from the $Ni^{+}(3d^{8}4d^{1})$ configuration.[20] In other cases, such a diffuse function has produced significant results, *e.g.* in $[Ni(NH_3)_4(NO_2)_2]$.[1]

Employing ASRED, again minimising $\Sigma[\sigma^2(I_o)]^{-1}(I_o - I_c)^2$, using all data, with fixed positional and thermal parameters, and with crystal electroneutrality constrained, we obtained for the 1 598 data with 95 variables $R(I) = 0.025$ with $R'(I) = 0.044$, and $\chi = 1.65$. The multipole populations and radii are listed in Table 7. Figure 4(*a*)—(*c*) shows the residual densities remaining. Figure 5(*a*)—(*c*) shows the difference between the multipole (calculated) density and the spherical theoretical atom density from the high-angle refinement, which is thus an estimate of the deformation density resulting from bonding changes.

Results and Discussion

Molecular Geometry and Thermal Parameters.—The nickel atom is approximately octahedrally co-ordinated by Cl(1), Cl(2) and four sulphurs related by the four-fold axis. The thiourea molecule, which is almost planar, is twisted with respect to the octahedral axes so that two sets of four N–H • • • Cl hydrogen bonds are made to hold the molecule in the crystal (Table 4). These hydrogen bonds are approximately linear.

The bond lengths and angles are in the normal ranges for Ni^{II} and thiourea complexes. We can compare the thiourea geometry with that of the 'free' molecule in the thiourea crystal.[9,10] The C–S bond is 0.6 pm shorter and the C–N bond 1.1 pm longer in the 'free' molecule. Although these changes are the directions of shift expected, due to contribution of the valence-bond resonance hybrid Ni^{+}–S–C=N^{+} in the complex, they only differ by *ca.* 3—4σ.

The most notable feature of the structure is the long Ni–Cl(2) bond[3] and the shorter Ni–Cl(1) bond. This difference may be the result of 'intramolecular' hydrogen bonding to thiourea N–H bonds tending to shorten Ni–Cl(1), while the corresponding N–H • • • Cl bonds for Ni–Cl(2) are 'intermolecular'. In the latter case, the direction of the hydrogen-bonding interaction would tend to lengthen the Ni–Cl(2) bond.

The thermal vibration parameters, $\bar{U}$, of the nickel, chlorine, and sulphur atoms at 140 K lie between 110 and 150 pm^2, with the exception of $U_{11}(U_{22})$ for Cl(2) which is much higher at 210 pm^2. The C motions are larger than for S and those for N larger again, appearing to reflect a situation in which the sulphur is tightly bound, whereas the end of the molecule containing the H atoms is more free to move. The N motions at 140 K (up to $\bar{U}$ = 470 pm^2) are not small. However, if we calculate the quantity $\Sigma(U_{ii}^{140}/U_{ii}^{295})$, and the e.s.d. of this ratio, we obtain values of 0.48(1) for the Ni, Cl, and S atoms and 0.46(2) for the C and N atoms. For a crystal showing harmonic motion, and well above its Debye temperature, we expect a value of 140/295 = 0.47. If the motion of all the non-hydrogen atoms is harmonic we thus have an internal check on our temperature calibration. For the hydrogen atom this ratio is much larger. This may be due to the fact that, for hydrogen atoms, the $\bar{U}$ values are not connected with motion of *core* electrons and are grossly affected by valence effects. An additional reason is the high zero-point motions associated with hydrogen atoms (*ca.* 150 pm^2) which has been experimentally demonstrated in the complex [Fe(bipy)Cl_3] (bipy = 2,2′-bipyridine).[21]

Qualitative Discussion of Deformation Electron Density.—The deformation densities shown in Figure 2(*a*)—(*c*) already show a number of interesting features, even if we allow for a corrupting effect caused by the use of the model phases in this non-centrosymmetric crystal.

In the thiourea fragment we observe, in Figure 2(*c*), peaks of 240 and 350 e nm^{-3} in the C–N bonds centred at 45 and 51 pm from N(1) and N(2) respectively. These C–N bonding peaks, besides being closer to N than C(1), are also asymmetric, being elongated towards the nitrogens. There is a bonding peak of 330 e nm^{-3} along the C–S bond centred 81 pm from C(1). There is also a slight build-up of density on the sulphur reflecting an increase in valence density or contraction in its radius. Since errors in such difference maps are large where densities are large, only valence-electron refinements will determine if this is an artefact or not. In addition we observe a 'lone-pair' peak of 290 e nm^{-3} at 90 pm from the sulphur approximately at right

Table 7. Multipole coefficients and radii from multipole refinement

Multipole	Ni(1) (3*d*)	Ni(1) (diffuse)	Cl(1)	Cl(2)	S(1)	C(1)	N(1)	N(2)	H(1)	H(2)	H(3)	H(4)
00	7.47(6)	2.69(27)	7.78(11)	7.17(11)	6.06(12)	3.96(14)	5.60(14)	5.72(14)	0.59(4)	0.57(6)	0.52(5)	0.67(6)
10	−0.3(1)	0.5(3)	0.2(1)	0.2(1)	—	—	—	—	0.0(1)	0.1(1)	0.1(1)	0.0(1)
11	—	—	—	—	0.3(1)	0.2(1)	0.1(1)	0.1(1)	—	—	—	—
1–1	—	—	—	—	0.3(1)	0.2(1)	0.1(1)	0.0(1)	—	—	—	—
20	0.0(1)	0.1(3)	0.0(2)	0.1(2)	0.1(1)	0.4(1)	0.2(1)	0.2(1)	0.1(1)	0.0(1)	0.0(1)	0.0(1)
22	—	—	—	—	0.0(1)	0.1(1)	0.0(1)	0.1(1)	—	—	—	—
2–2	—	—	—	—	0.01(1)	0.1(1)	0.0(1)	0.2(1)	—	—	—	—
30	0.5(2)	2.3(3)	0.2(2)	0.2(2)	—	—	—	—	—	—	—	—
31	—	—	—	—	0.2(1)	0.0(2)	0.4(1)	0.0(1)	—	—	—	—
3–1	—	—	—	—	0.0(1)	0.2(2)	0.5(2)	0.1(1)	—	—	—	—
33	—	—	—	—	0.2(1)	0.8(2)	1.0(1)	0.9(1)	—	—	—	—
3–3	—	—	—	—	0.0(1)	0.1(2)	0.0(1)	0.0(1)	—	—	—	—
40	0.01(2)	—	0.3(2)	0.2(2)	0.0(1)	—	—	—	—	—	—	—
42	—	—	—	—	0.3(1)	—	—	—	—	—	—	—
4–2	—	—	—	—	0.0(1)	—	—	—	—	—	—	—
44	0.8(3)	—	0.3(4)	0.3(4)	0.5(1)	—	—	—	—	—	—	—
4–4	0.3(3)	—	0.1(4)	0.4(3)	0.1(1)	—	—	—	—	—	—	—
Radius	1.01(1)	—	0.99(2)	0.98(2)	0.95(1)	1.01(2)	1.02(1)	1.01(1)	—	—	—	—

angles to the C–S bond, also directed approximately at the nickel atom. Most of these features also appear with similar heights and positions on analogous $X-X_{high\ angle}$ maps for the thiourea crystal.[10] We note that our use of refined hydrogen positions will flatten any features in the N–H bonds, such as those observed in thiourea where hydrogen nuclear (neutron diffraction derived) co-ordinates are used. This agreement, particularly in C–N and C–S bonding peaks, is encouraging since we expect these to be little affected by co-ordination to nickel. Although detailed comparison must wait until the effects of incorrect phasing are minimised by better modelling, and until we extract *static* rather than *dynamic* valence features, one effect of nickel bonding is already apparent. There are no longer two symmetrical 'lone-pair' peaks on each side of the sulphur in the thiourea plane. This 'lone-pair' can also be seen in Figure 2(*b*) in the Ni–S bond. In Figure 2(*a*) we can also see some excess density on the $+z$ side of Cl(1) and Cl(2), perhaps indicating a polarisation of σ-symmetry density in these atoms.

Around the nickel atom we observe a hole of depth −500 e nm^{-3} at 50 pm from the nickel, a hole of −240 e nm^{-3} at 130 pm along the Ni–Cl(2) direction, and along the Ni–Cl(1) direction a hole of −390 e nm^{-3} at 110 pm from the nickel. In this plane there are no peaks but in the NiS_2 plane we observe four peaks of height 300 e nm^{-3} at 90 pm from the nickel. In addition there is a hole of −300 e nm^{-3} at 40 pm from nickel along the Ni–S bond. This 'hole' is more accurately described as a trough connecting to the large hole along Ni–Cl(2): the negative region is therefore a deep hole with four finger-like extensions reaching up to the Ni–S axis [see Figure 2(*a*)]. The general pattern of peaks and troughs is as expected for a d^8 Ni^{II} ion in a tetragonal crystal field: holes along the nickel–ligand axis at *ca.* 50 pm from the nickel and positive density elsewhere peaking between the ligand axes. However, a simple crystal-field model predicts an equality of all holes and peaks which we do not observe. The inequality is presumably caused by differing charge transfers from chlorines and thiourea as well as perhaps the differential occupation of 4*s*/4*p* orbitals. Such speculation can only be confirmed by the quantitative modelling whose results we present next.

Valence Model Refinement.—(*a*) *Charge transfers.* In Table 6 we list the net charges obtained in the valence model refinement. The charges within the thiourea molecule show substantial deviations from neutral atoms, presumably reflecting the strong bonding within the free molecule rather than effects of metal ligation. The atomic charges within the $-NH_2$ fragments, in particular, should not be compared in detail with theoretical calculation since the 'hydrogen' charge is not fixed at the true nuclear position. It is well known that the charge centroid is shifted about 20 pm into a X–H bond. The charge assignments for Ni, mean Cl, and total thiourea are meaningful, particularly the last since the weaker bonding and longer Ni–S bonds allow a more precise division of electron density which is less affected by overlap. We obtain a charge of +0.17(20) on each thiourea molecule. There has been a transfer of 0.17(20) e from each thiourea molecule, 0.52(18) e from the 'mean' chlorine, and the nickel has a net charge of +0.3(2). These three numbers agree in suggesting that the four thiourea molecules donate less [0.7(4)] than only two chlorine ligands [1.0(4)].

(*b*) *Thiourea molecule.* Examination of the results of the anisotropic refinement shows that, apart from S(1), there is mirror symmetry across the plane defined by the C–S bond and the perpendicular to the thiourea molecule, just as in the free molecule. To make a comparison with the free molecule we can transform the four sp^3 hybrids on sulphur into $3sp^2 + p$ with some neglect of higher multipoles. We obtain a p_π population on sulphur of 0.5 e, giving a total molecular π population of 4.25(14). This is hardly different from the value of 4 expected for the free molecule on simple molecular orbital (m.o.) grounds. This explains the substantial anisotropy around C(1), where the p_π population seems very low, and the similar smaller anisotropy around N(1) and N(2). However, the effect of ligation of the nickel is evident at the sulphur. If we assume a π-plane as above, we obtain one sp^2 population [that pointing neither at C(1) nor Ni(1)] as 2.8(1) e. This is obviously an unphysical result for an sp^2 'lone-pair'. The assumption of sp^3 hybrids allows us to fit the atom S(1) with all populations less than 2. If we approximate the molecule as simple m.o.s constructed from hybridised atoms we deduce that the nickel has a sufficiently strong effect on the thiourea to produce two sp^3 hybridised 'lone-pairs'. This strong nickel–thiourea interaction contrasts with the observed very small charge transfer.

(*c*) $NiCl_2$ *fragment.* The observed mean σ and π chlorine populations [3.84(14)σ + 3.65(15)π] can be compared with a free *sp* polarised chloride ion (4σ + 4π), and indicate both σ and π donation to the nickel atom, totalling 0.33(28)σ and 0.70(30)π respectively. The nickel 3*d* configuration, $3d_{x,y}^{1.91(14)}$ $3d_{xz,yz}^{3.08(18)}$, $3d_{x^2-y^2}^{1.12(14)}$ $3d_{z^2}^{1.39(14)}$, resembles the high-spin configuration expected from a simple tetragonal crystal field, $3d_{xy}^2$ $3d_{xz,yz}^4$ $3d_{x^2-y^2}^1$ $3d_{z^2}^1$. There are however significant differences. The $3d_{z^2}$ and $3d_{x^2-y^2}$ populations imply gain in σ

population of 0.40 e from each thiourea and 0.17 e from each chlorine. A simple $3d$ system is of course by symmetry unable to distinguish between gains from Cl(1) or Cl(2). The $3d_{xy}$ population of 1.91(14) is insignificantly different from 2, implying no strong π effects from the thiourea, while the $3d_{xz,yz}$ population, which is of π symmetry in the $NiCl_2$ fragment, differs from the crystal-field prediction by 0.92(18) e. The $3d$ configuration on the nickel therefore agrees with the ligand populations in ascribing little σ or π charge transfer from thiourea while Cl(1) + Cl(2) have substantial changes in both σ and π, σ being the smaller. The mean chlorine ligand σ donation of 0.33 e matches the 0.34 e gain observed in the appropriate σ symmetry nickel $3d_\sigma$ orbitals. However, for the π electrons the π donation of 0.70 e *from* the chlorine is observed together with a *decrease* of 0.92 e on the nickel $3d_\pi$. In a simple linear combination of atomic orbitals m.o. picture the interaction between filled Cl π orbitals and filled nickel $3d_\pi$ orbitals produces only small population changes associated with the net overlap density. In this case a large $4p_\pi$ population [1.6(7) e] has appeared on the nickel. It appears that there is substantial $4p$ participation in the π bonding, while conversely, and as the charge transfers imply, the nickel $4p_\sigma$ population of 0.6(5) e implies little $4p$ participation in the σ bonding. It is encouraging to note the precisely similar situation that we observed in $[Ni(NH_3)_4(NO_2)_2]$.[1] The strongly σ-bonding NO_2^- group donated into the $3d_\sigma$ orbitals, as did the rather weaker σ-bonding NH_3 groups. However, the $3d_\pi$ orbital on the nickel, and possibly (at only the 2σ significance level) the NO_2^- π orbitals both lost π-electron density which appeared in a $4p$ orbital of π symmetry with respect to the $Ni(NO_2)_2$ plane. Since this unexpected result for the π electrons has now appeared again here it is less likely to be an artefact or accident. In both these experiments we have labelled and modelled the more diffuse functions as $4p$. In both cases using $4s$ functions could produce the same effect, or indeed so could a differential nephelauxetic effect amongst the angularly different $3d$ orbitals. Given that the nodal behaviour near the nucleus is experimentally inaccessible the choice is, at this stage, a matter of taste. The conclusion of an expanded π distribution is not.

While the broad σ- and π-bonding features described thus far conform to a relatively simple isolated $NiCl_2$-fragment model the sp-hybrid populations on Cl(1), N(1), and Cl(2) do not. The polarisation differences between the $-z$ and $+z$ hybrids are 0.58(15) for the mean chlorine and 1.0(6) for nickel. This polarisation of the relatively diffuse $3sp$ and $4sp$ atomic orbital populations all in the same direction is difficult to explain simply as a consequence of bonding in an isolated $NiCl_2$ fragment. It seems more likely to be a result of long-range crystal-field effects from the rest of the crystal.

(*d*) *Residual density maps.* The residual densities are shown in Figure 3(*a*)—(*c*). The general improvement in fit over the spherical atom model [Figure 2(*a*)—(*c*)] is evident: for example, the areas of |density| > 200 e nm^{-3} are reduced by a factor of *ca.* 3.

In the thiourea fragment [Figure 3(*c*)] the bonding features in the C–S and C–N bonds while still present are much reduced in height. It appears that this bonding density can be significantly projected into sp hybrids (up to second-order multipoles), although for complete projection it is known that at least third-order multipoles are necessary.[9] The 'lone-pair' along the S–Ni direction is not well modelled by the valence orbitals used, as it shows sharper features than a simple sp hybrid. Figure 3(*a*) shows that the chlorines are adequately modelled by sp hybrids. The most significant areas remaining on this map are the holes approximately midway along both Ni–Cl bonds. The valence modelling has removed density of nickel origin, showing that these holes are of equal magnitude at the same points along each Ni–Cl bond (−280 e nm^{-3} at 115 pm from the nickel). The sulphur 'lone-pair' is again evident in both Figure 3(*a*) and (*b*) along the Ni–S bonds. The only remaining residual density of significance is around the nickel. Figure 3(*a*) and 3(*b*) shows that the $3d + 4sp$ hybrids have modelled the complex hole along the Ni–Cl(2) bond stretching up to the Ni–S bond quite well. There is a slight suggestion from the remaining asymmetry along the $NiCl_2$ direction that this is not a complete explanation. The most important residual densities are shown in Figure 3(*b*) and are the four peaks of 270 e nm^{-3} at 90 pm from the nickel. These peaks are at 22° to the Ni–S axis. While the C–N, C–S, and 'lone-pair' densities are easily explained, these four peaks and the two holes along the Ni-Cl bonds, all at *ca.* 100 pm from the nickel, are of less obvious origin. The four peaks *could* be modelled in terms of $4d$ orbitals, with substantial $4d_{xy}/4d_{x^2-y^2}$ mixing to explain the 22° angle. Alternatively, we could invoke a 'differential nephelauxetic effect', expanding $3d_{xy}$ more than $3d_{x^2-y^2}$; Figure 2(*b*) lends plausibility to this. The angular change (from 45 to 22°) could again be accommodated by mixing.

Whatever theoretical explanation is used we can say that the non-bonded (t_{2g}^6) electron density is expanded relative to the σ-bonded e_g^2. Also, the angular change from 45 to 22° shows that simple σ bonding *via* the $NiCl_2S_4$ distorted octahedron is not an adequate explanation: the nickel atom is sensitive to the remainder of the crystal. The holes along the Ni–Cl_2 axis can also be explained as a contraction of the σ-bonded nickel density, or a $4d_{z^2}$ relatively empty compared to other $4d$ orbitals. Such a contraction could arise equally from a 'differential nephelauxetic effect' or from the orthogonalisation of Cl and Ni orbitals which is theoretically necessary even in the absence of any other bonding effects. Of course, these two explanations are opposite extremes of a continuum, reflecting assumptions of the balance between exchange and Coulomb integrals in the m.o. picture. The validity of the assumptions can only be examined by theoretical calculations. This is equally true of the $4d/3d$ balance and its effect on the four peaks and two holes around the nickel.

Multipole Refinement.—The improvement in χ from 1.78 to 1.65 over the valence model is significant, although less than we might initially have expected. The residual Fourier maps [Figure 4(*a*)—(*c*)] show little change in the $NiCl_2$ fragment, but a noticeable improvement in the thiourea molecule, especially around the sulphur atom. The asphericity observed in the valence refinements is broadly similar in the multipole refinements. There are 10 multipoles significant at 2.5σ or greater. Of these the multipoles Ni(1) [44], Cl(1) [10], S(1) [10,11], (C(1) [20], Ni(diffuse) [30] show the same asphericity as observed for these atoms in the valence refinements, which have already been interpreted in chemical terms; [*ml*] indicates the multipole associated with the spherical harmonic Y_l^m. For example, Ni(1) [44] represents a significant ($3d_{xy} - 3d_{x^2-y^2}$) population difference. In all cases the asphericity is more strongly determined in the valence model than multipole model. This is probably due to the doubling of parameters causing the multipole model to be over-parameterised given the data quality. Within the rationale of the multipole model this is necessary, however, since we see five higher-order multipoles not taken into account in the valence model {S(1) [44], C(1) [3,3], N(1) [31,33], and N(2) [33]} which have significant populations. These multipoles cause density to be placed in the bond connecting to the other atoms [Ni–S–C(1)(tetrahedral approx.), N(1)(trigonal), N(2)(trigonal), and C(1)(trigonal)], as shown in Figure 5. These higher multipole coefficients are well known to perform the function of modelling 'mid-bond' densities, so this result is expected. The improvement in the density maps of the thiourea fragment, and the uncharged $NiCl_2$, is another reflection of this result.

The deformation density of thiourea [Figure 5(*c*)] resembles

that found for free thiourea[9,10] quite closely, showing that, as the quantitative results and all previous chemical experience show, the changes in most ligands on complexation are small. We observe higher peaks in the C–N and C–S mid-bond region than in Figure 2(*c*), reflecting the improvement in model phases. The peak heights (500 and 400 e nm^{-3} respectively) compare well with the dynamic deformation densities observed in thiourea itself,[9,10] where the thermal parameters are comparable with the results of this experiment. We also agree in seeing 'lone pairs' close to the sulphurs in the thiourea plane, almost perpendicular to the C–S bond, of height *ca.* 200 e nm^{-3}. In our case the lone pair directed approximately along the Ni–S bond is at a slightly greater distance and is less well modelled than that of the uncomplexed molecule. This transfer of charge from the sulphur lone pair towards the nickel is expected. The asymmetry of 'lone pairs' in Figure 5(*c*) reflects the effect of nickel complexation. Figure 4(*a*) and (*b*) shows that the multipole density [Figure 5(*a*) and (*b*)] is a good representation of the density in the $NiCl_2$ fragment, apart from the 4*d* density already discussed. We note the substantial difference in nickel density along the Cl(1) and Cl(2) bonds. This is the same as in Figure 2(*a*), but deeper because of better phasing. However, we shall not discuss it further as the appropriate multipoles ([1,0] and [3,0]) have large errors, which again reflect the difficulty of separating the two Ni–Cl bonding parameters in this acentric structure.

Covalence, Diffraction, and Spectroscopy.—In octahedral symmetry the ground- and first-excited terms of $Ni^{II}(d^8)$ are $^3A_{2g}(F)$ and $^3T_{2g}(F)$. The $^3T_{2g}(F)$ term is split in tetragonal (C_{4v}) symmetry into ^3E and $^3B_2$ terms, while the ground term is relabelled as $^3B_1$. If we allow spin–orbit coupling then two excited terms each mix with *different* M_S components of the ground term to split it into E ($M_S = \pm 1$) and B_2 ($M_S = 0$) states. This zero-field splitting ($D = E_E - E_{B_2}$), since it depends on the mixing in of the higher states, will be positive if the E state is lower in energy than B_2.[5]

The anisotropy in the single-crystal magnetic susceptibilities gives $D = 7.6(4)$ K, with somewhat smaller intermolecular exchange.[7] This is consistent[5] with the assignment of bands at *ca.* 7 500 and 9 300 cm^{-1} to the $^3B_1 \rightarrow {}^3E$ and $^3B_1 \rightarrow {}^3B_2$ transitions respectively, as well as the *g*-tensor and expected spin–orbit coupling. This information, together with other higher-energy spectroscopic levels, can be satisfactorily interpreted in terms of a crystal-field model (*Dq*, *Ds*, *Dt*, *etc.*).[5] It implies an energy ordering of 3*d* levels in the Ni^{2+} ion in this complex of $3d_{x^2-y^2} > 3d_{z^2} > 3d_{xy} \approx 3d_{xz,yz}$.

Before we can examine the agreement of spectral and *X*-ray diffraction parameters we must extract individual bond parameters. From the spectroscopy and magnetism Gerloch *et al.*[5] have derived the relationship (1). To extract covalence parameters from the diffraction data we must examine the symmetry-

$$Dq(\mathrm{tu}) > \{Dq[\mathrm{Cl}(1)] + Dq[\mathrm{Cl}(2)]\}/2 \qquad (1)$$

adapted molecular orbitals for this MX_4YY' molecule. If we restrict ourselves to σ bonding involving metal 3*d* and ligand *sp* orbitals we have the two antibonding orbitals given below.

$$312|N_a^1\psi_a^1 = (1 - a_{tu}^2)^{\frac{1}{2}}|3d_{x^2-y^2}> - (a_{tu}/2)(|sp_{tu1}> - |sp_{tu2}> + |sp_{tu3}> + |sp_{tu}>)$$

$$N_a^2\psi_a^2 = \left(1 - \frac{a_{tu}^2}{3} - \frac{a_{Cl(1)}^2}{3} - \frac{a_{Cl(2)}^2}{3}\right)|3d_{z^2}> - (a_{tu}/\sqrt{12})(-|sp_{tu1}> - |sp_{tu2}> - |sp_{tu3}> - |sp_{tu4}>) - (2/\sqrt{12})(a_{Cl(1)}|sp_{Cl(1)}> + a_{Cl(1)}|sp_{Cl(2)}>)$$

The valence analysis of the *X*-ray data show charge transfers from ligand σ framework to metal for all ligands and a gain in both $3d_{z^2}$ and $3d_{x^2-y^2}$ as expected. The σ framework ligand charge losses are 0.16 and 0.17 for each mean chlorine and thiourea respectively and the gains 0.39 and 0.12 respectively for $3d_{z^2}$ and $3d_{x^2-y^2}$. Although the e.s.d.s on these numbers render them only just significant even at the 2σ level, when taken together they give a consistent estimate of equation (2). The

$$\tfrac{1}{2}(a_{Cl(1)} + a_{Cl(2)}) \simeq a_{tu} \qquad (2)$$

relationships (1) and (2), which summarise the essence of the spectral and diffraction data, are on the surface contradictory, insofar as *Dq* is related to the strength of M–L bonding. To understand that this is not so we use a simple m.o. model.

Within the framework of the Wolfsberg–Helmholtz model[8,22] we can write for a diatomic M–L molecule an antibonding molecular orbital of energy E_a considering only σ-bonding, equation (3), and with a wavefunction given by equation (4),

$$E_a = H_M + \frac{(H_L S_{ML})^2}{(H_M - H_L)} \qquad (3)$$

$$N_a\psi_a = (1 - a_L^2)^{\frac{1}{2}}|\psi_M> - a_L|\psi_L> \qquad (4)$$

where $a_L \simeq -H_L S_{ML}/(H_M - H_L)$ for small a_L. In these equations a_L is the ligand covalence coefficient, while $|\psi_M>$ and $|\psi_L>$ are suitable atomic wavefunctions, and H_M and H_L valence-state ionisation energies for metal and ligand respectively. S_{ML} is the diatomic overlap integral and N_a the normalising factor. To explain the spectral and diffraction results we must estimate the H and S values. The Hartree–Fock atomic wavefunctions for Ni^{2+}, S, and Cl^- are used, in the guise of form factors, with great success in the refinement of the *X*-ray data. These form factors show that S is slightly larger than Cl^-. With the bond lengths in Table 3 we can estimate equation (5). The ionisation

$$S_{NiS} \simeq 0.3 \simeq S_{NiCl(1)} > S_{NiCl(2)} \simeq 0.15 \qquad (5)$$

energy of Cl^- is *ca.* 4 eV while that of thiourea is *ca.* 10 eV. Conventionally $H_M > H_L$, because of the larger spherical 'crystal field' potential, and the observed lack of substantial L ⟶ M charge transfer. Therefore we estimate equation (6). If

$$0 > H_M > H_{Cl} \simeq 4 \text{ eV} > H_{tu} \simeq -10 \text{ eV} \qquad (6)$$

we assume $H_M \simeq -2.5$ eV, a not unreasonable figure, we can calculate from equation (4) and the values in equations (5) and (6), equation (7). Similarly, from equation (3), we can calculate

$$a_{Cl(1)} = 0.8 > a_{Cl(2)} = 0.4 = a_{tu} \qquad (7)$$

$$Dq(\mathrm{tu}) = 1.2 > Dq[\mathrm{Cl}(1)] = 0.96 > Dq[\mathrm{Cl}(2)] = 0.24 \qquad (8)$$

equation (8). The relationships (7) and (8), derived from bond lengths, form factors, and ionisation potentials are in excellent agreement with equations (1) (from spectral data) and (2) (valence analysis of *X*-ray diffraction). We can now see that the inversion of thiourea and chloride effects is due to the competing influences of $H_L S_{ML}$ and $(H_M - H_L)$, which become $|H_{Ni} - H_{Cl}| < |H_{Ni} - H_{tu}|$ and $|H_{Cl}S_{NiCl}| < |H_{tu}S_{NiS}|$.

Although we have used the Wolfsberg–Helmholz model, the same qualitative trends may be derived from simple qualitative arguments balancing the effects of overlap and orbital energies. The Wolfsberg–Helmholz model is sufficiently crude that we should pay little attention to specific numerical predictions. A

more realistic *ab-initio* or X-α calculation would, we hope, illustrate the point more convincingly, maybe even quantitatively.

We have pursued this argument in some detail because the quality of the experimental data warrants it. However, in general terms, it is already well known[23] that the *energy levels* are dominated by the effects of the orthogonalisation of pure metal and ligand orbitals (overlap). In relatively ionic bonds the covalence or electron delocalisation over the metal and ligands has a secondary effect. This crystal is therefore an excellent example of the fact that covalence (*a* terms in our model) is most easily determined by experiments sensitive to electron density (*X*-ray diffraction, e.s.r., polarised neutron diffraction), and not by those probing energies (spectra, magnetism).

Acknowledgements

Our thanks are due to the Australian Research Grants Scheme for financial support, and to the Crystallography Centre, University of Western Australia, in particular Associate Professor A. H. White for undertaking the data collection.

References

1 B. N. Figgis, P. A. Reynolds, and S. Wright, *J. Am. Chem. Soc.*, 1983, **105**, 434.
2 B. N. Figgis, P. A. Reynolds, and R. Mason, *J. Am. Chem. Soc.*, 1983, **105**, 440.
3 A. Lopez-Castro and M. R. Truter, *J. Chem. Soc.*, 1963, 1309.
4 M. Nardelli, L. Cavalca, and A. Braibanti, *Gazz. Chim. Ital.*, 1956, **86**, 942.
5 M. Gerloch, J. Lewis, and W. R. Smail, *J. Chem. Soc. A*, 1971, 2434.
6 C. J. Ballhausen and C. R. Hare, *J. Chem. Phys.*, 1964, **40**, 788.
7 A. Paduan-Filho, R. D. Chirico, K. D. Joung, and R. L. Carlin, *J. Chem. Phys.*, 1981, **74**, 4103.
8 M. Gerloch and R. C. Slade, 'Ligand Field Parameters,' Cambridge University Press, 1973.
9 D. Mullen, *Acta Crystallogr., Sect. B*, 1982, **38**, 2620.
10 A. Kutoglu, C. Scheringer, H. Meyer, and A. Schweig, *Acta Crystallogr., Sect. B*, 1982, **38**, 2626.
11 D. W. J. Cruickshank, *Acta Crystallogr.*, 1950, **3**, 72.
12 J. M. Stewart, 'The X-RAY System—Version of March 1976,' Technical Report TR-446, Computer Science Centre, University of Maryland, U.S.A.
13 D. T. Cromer and J. B. Mann, *Acta Crystallogr., Sect. A*, 1968, **24**, 321.
14 R. F. Stewart, E. R. Davidson, and W. T. Simpson, *J. Chem. Phys.*, 1965, **42**, 3175.
15 D. T. Cromer and D. J. Liberman, *J. Chem. Phys.*, 1970, **53**, 1891.
16 'International Tables for *X*-Ray Crystallography,' Kynoch Press, Birmingham, 1979, vol. 4, pp. 102—147.
17 B. N. Figgis and P. A. Reynolds, unpublished work.
18 E. U. Condon and G. H. Shortley, 'The Theory of Atomic Spectra,' Cambridge University Press, 1957.
19 F. L. Hirshfeld, *Acta Crystallogr., Sect, B*, 1971, **27**, 769.
20 E. Clementi and C. Roetti, *At. Data Nucl. Data Tables*, 1974, **14**, 177.
21 B. N. Figgis, P. A. Reynolds, and N. Lehner, *Acta Crystallogr., Sect. B*, 1983, **39**, 711.
22 M. Wolfsberg and L. Helmholz, *J. Chem. Phys.*, 1952, **20**, 837.
23 C. J. Ballhausen, 'Molecular Electronic Structure of Transition Metal Complexes,' McGraw-Hill, New York, 1979, pp. 38—61.

Received 11*th December* 1984; *Paper* 4/2102